feature was visible near the expected locations. The 3-σ upper limit to the disk-integrated *I/F* of any undetected satellite, derived from individual 120-s exposures, is 30 km^2 (*3*). For comparison, Mab had a disk-integrated *I/F* of 50 km^2 in the HST data, while near maximum elongation as in our October images. This moon is thus very dark near 2 μm, suggestive of absorption by water ice. This makes Mab comparable in surface composition to the five "classical" moons Miranda through Oberon, whose spectra show deep (factor 2 to 3) water ice absorption features near 2 μm. In contrast, Uranus's small inner moons are neutral to slightly red throughout the visual-infrared (*6*, *7*), suggesting that water ice is absent from their surfaces. Mab orbits midway between these two populations. Because of its tiny size, Showalter and Lissauer (*1*) assumed that Mab would resemble the inner moons, with a small geometric albedo (7 to 10%). Our data suggest that Mab may be covered by ice and therefore be as bright as the outer moons (albedo 20 to 40%). This would decrease Mab's estimated radius from 12 km to 6 to 8 km and hence means that Mab, rather than Cupid (~8 km), is Uranus' smallest regular satellite.

In 2007, Uranus' ring system will appear edge-on to Earth, making faint rings ~100 times brighter and enabling measurements of their vertical extent. If indeed similar physical processes are at work within R1 as in Saturn's E ring, then particles in R1 must also be subject to vertical perturbations, resulting in a vertically extended ring. This can be verified in 2007.

References and Notes

1. M. R. Showalter, J. J. Lissauer, *Science* **311**, 973 (2006).
2. I. de Pater, S. G. Gibbard, H. B. Hammel, *Icarus* **180**, 186 (2006).
3. Materials and methods are available as supporting material on *Science* Online.
4. J. A. Burns, D. P. Hamilton, M. R. Showalter, in *Interplanetary Dust*, E. Grün, B. A. S. Gustafson, S. F. Dermott, H. Fechtig, Eds. (Springer-Verlag, Berlin), pp. 641–725 (2001).
5. R. G. French, P. D. Nicholson, C. C. Porco, E. A. Marouf, in *Uranus*, J. T. Bergstrahl, E. D. Miner, M. S. Matthews, Eds. (Univ. Arizona Press, Tucson), pp. 327–409 (1991).
6. E. Karkoschka, *Icarus* **151**, 51 (2001).
7. S. G. Gibbard, I. de Pater, H. B. Hammel, *Icarus* **174**, 253 (2005).
8. M. R. Showalter, J. N. Cuzzi, S. M. Larson, *Icarus* **94**, 451 (1991).
9. I. de Pater, S. C. Martin, M. R. Showalter, *Icarus* **172**, 446 (2004).
10. M. M. Hedman *et al.*, *BAAS* **37** #66.02 (2005).
11. M. R. Showalter, J. N. Cuzzi, *Icarus* **103**, 124 (1993).
12. H. B. Throop, L. W. Esposito, *Icarus* **131**, 152 (1998).
13. J. A. van Allen, M. F. Thomson, B. A. Randall, R. L. Rairden, C. L. Grosskreutz, *Science* **207**, 415 (1980).
14. T. Johnson, American Geophysical Union, Fall Meeting, San Francisco, 5–9 December 2005, P21F-03.
15. M. Horanyi, J. A. Burns, D. P. Hamilton, *Icarus* **97**, 248 (1992).
16. A. Juhász, M. Horányi, *J. Geophys. Res.* **107**, 1 (2002).

17. This work was funded by the National Science Foundation and Technology Center for Adaptive Optics, managed by the University of California at Santa Cruz under cooperative agreement AST-9876783. The W. M. Keck Observatory is operated as a scientific partnership among the California Institute of Technology, the University of California, and the National Aeronautics and Space Administration and was built with financial support of the W. M. Keck Foundation. Further support was provided by NASA grants NAG5-11961 and NAG5-10451 (H.B.H.), NNG05GL48G (M.R.S.), and proposal numbers GO-9823, 10102, and 10274 from the Space Telescope Science Institute, operated by the Association of Universities for Research in Astronomy, under NASA contract NAS5-26555. S.G.'s work was performed under the auspices of the U.S. Department of Energy, National Nuclear Security Administration, by the University of California, Lawrence Livermore National Laboratory under contract W-7405-Eng-48.

Supporting Online Material

www.sciencemag.org/cgi/content/full/312/5770/92/DC1
Materials and Methods
References

18 January 2006; accepted 2 March 2006
10.1126/science.1125110

Deconvolution of the Factors Contributing to the Increase in Global Hurricane Intensity

C. D. Hoyos,* P. A. Agudelo, P. J. Webster, J. A. Curry

To better understand the change in global hurricane intensity since 1970, we examined the joint distribution of hurricane intensity with variables identified in the literature as contributing to the intensification of hurricanes. We used a methodology based on information theory, isolating the trend from the shorter-term natural modes of variability. The results show that the trend of increasing numbers of category 4 and 5 hurricanes for the period 1970–2004 is directly linked to the trend in sea-surface temperature; other aspects of the tropical environment, although they influence shorter-term variations in hurricane intensity, do not contribute substantially to the observed global trend.

Recent publications linking an increase in hurricane intensity to increasing tropical sea-surface temperatures (SSTs) (*1*–*5*) have fueled the debate on whether global warming is causing an increase in hurricane intensity (*6*, *7*). The arguments associating the increase in hurricane intensity with increasing SSTs (*1*) note positive trends in both global tropical SST and the number of category 4 and 5 hurricanes (NCAT45). The physical mechanism linking the increases in tropical SST and NCAT45 is the theory of maximum potential intensity (*3*).

School of Earth and Atmospheric Sciences, Georgia Institute of Technology, Atlanta, GA 30332, USA.

*To whom correspondence should be addressed. E-mail: choyos@eas.gatech.edu

The analysis presented in (*1*) established the existence of coincident positive trends of tropical SST and NCAT45 in each of the ocean basins. Outstanding issues in understanding the substantial increase in global NCAT45 since 1970 include (i) identification of the contributions of natural internal variability on decadal and shorter time scales as compared to a longer-term trend and (ii) identification of the importance of SST in causing the increase in NCAT45, relative to other known variables that influence hurricane intensity (*8*, *9*).

To address these issues, we analyzed the time series of SST, specific humidity in the layer extending from 925 to 500 millibars (mb), wind shear between 850 and 200 mb, and the 850-mb zonal stretching deformation (the change of zonal wind with longitude). Increasing SST, increasing specific humidity, minimal vertical wind shear, and negative stretching deformation are associated with increasing hurricane intensity. The data sets used in this analysis were the hurricane data set described in (*1*), the National Oceanic and Atmospheric Administration Extended Reconstructed SST data set (*10*), and the National Centers for Environmental Prediction/National Center for Atmospheric Research Reanalysis (*11*). The analysis was conducted for seasonally averaged values for the period 1970–2004 for global hurricanes, including data from the North Atlantic (NATL), West Pacific (WPAC), East Pacific (EPAC), South Pacific (SPAC), South Indian (SIO), and North Indian (NIO) Oceans. Hence, the data set consisted of data points for 35 seasons and six different ocean basins, for a total sample size of 210.

Figure 1 shows a clear positive trend in SST in each of the ocean basins. Although there is no consistent global trend of specific humidity, wind shear, and stretching deformation, there are statistically significant trends [as per the Mann-Kendall approach (*12*)] in several of the basins (Table 1): in the EPAC, a positive trend in specific humidity; in the SPAC, a negative trend in stretching deformation at 850 mb; and in the NATL, a negative trend in wind shear. It is important to note that these particular trends reinforce the necessary conditions for hurricane formation. The SST trends are not only statistically significant in each of the ocean basins but also have the largest magnitude, except for the SPAC, where stretching defor-

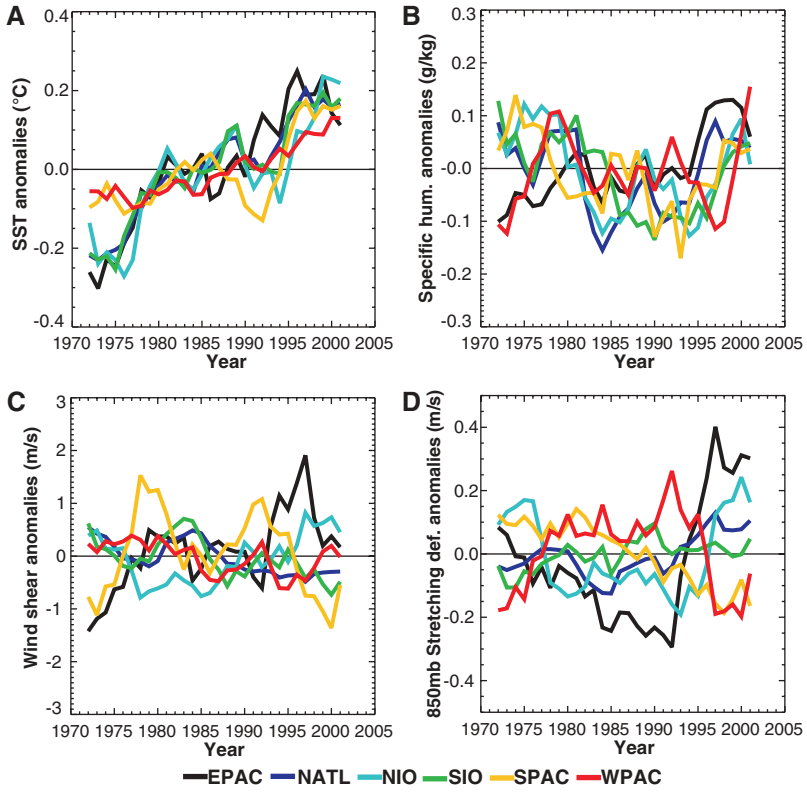

Fig. 1. Five-year moving average anomalies relative to the 1970–2004 period for the EPAC (90° to 120°W, 5° to 20°N, June-October), NATL (90°W to 20°E, 5° to 25°N, June-October), NIO (55° to 90°E, 5° to 20°N, April-May and September-November), SIO (50° to 115°E, 5° to 20°S, November-April), SPAC (155° to 180°E, 5° to 20°S, December-April), and WPAC (120° to 180°E, 5°to 20°N, May-December). Basins and seasons are defined by (*1*) for (**A**) SST, (**B**) specific humidity, (**C**) wind shear, and (**D**) stretching deformation at 850 mb.

Table 1. Standardized trends (per 35 years) for all variables in each basin for the period 1970–2004.

Basin	SST	Specific humidity	Wind shear	Stretching deformation (850 mb)
EPAC	1.934*	1.228*	0.827	0.581
NATL	2.767*	0.058	−1.880*	1.208
NIO	2.017*	−0.971	0.315	−0.134
SIO	2.095*	−0.653	−1.468	0.734
SPAC	1.788*	−0.159	−0.035	−1.840*
WPAC	2.046*	0.803	−0.562	0.376

*Values are significantly different than zero at the 99% confidence level.

mation at 850 mb also presents a trend of comparable magnitude.

To understand the relationships between NCAT45 and the four variables considered, we used a methodology based on information theory, whereby the mutual information (MI) of both variables is quantified to represent the measure of independence of the two variables (*13*). Specifically, the MI quantifies the distance between the joint distribution of two variables, X and Y, and the product of their marginal distributions. MI can be thought of as a measure of the information of X that is shared by Y. If X and Y are independent, then X contains no information about Y and vice versa, so their MI is zero [see supporting online material (*14*)].

To quantify the MI, it is necessary to estimate the marginal distribution of the variables. Figure 2, A and B, shows the distributions of NCAT45 and SST. If these two variables were statistically independent, the product of their marginal distributions should replicate their joint distribution (Fig. 2C). The fact that this is not seen for NCAT45 and SST implies that there is statistical dependence between the variables. The joint distribution (Fig. 2D) indicates that statistically, the average SST during each basin's hurricane season should be high in order to have a larger value of NCAT45. That is, high SST is important not only during the lifetime of a single event (*15*, *16*), but the average SST conditions of the basin seem to be highly linked with the probability of occurrence of NCAT45. The scaled distribution [the joint distribution scaled by the marginal distribution (Fig. 2E)] shows that higher values associated with their MI [0.51 bits (*17*)] are located along the diagonal and mainly in its upper part, confirming that the seasonal values of SST are intimately related to NCAT45.

To address the issue of the relative importance of the MI between NCAT45 and SST versus the other variables, we performed the same MI statistical analysis. For specific humidity (Fig. 3A), the analysis indicates that the MI is 0.49 bits. Higher seasonal average values of specific humidity are associated with higher values of NCAT45, with no high NCAT45 associated with low values of specific humidity. Wind shear (Fig. 3B) also shows a relationship with NCAT45 (0.44 bits), with values associated with high values of NCAT45 in the bottom half of the distribution. In other words, high NCAT45 is more likely to occur when the wind shear tends to be low relative to its distribution. In the case of stretching deformation (Fig. 3C), it is clear that the occurrence of high NCAT45 always corresponds to negative values of stretching deformation (*9*) and explains most of the MI, which is 0.68 bits.

The values of the MI presented in Figs. 2 and 3 are roughly comparable in magnitude, ranging from a high value of 0.68 bits for stretching deformation to a low value of 0.44 bits for wind shear. Because this analysis does not directly allow for distinguishing whether these relationships arise from the long-term trend or the shorter-term modes of natural internal variability (on a decadal scale or shorter), we performed the MI analysis on the isolated trend/variability time series (*14*). The trend is removed by subtracting the least-squares linear fit from each basin's variable time series. This method has a physical interpretation only if the trend has a consistent sign in all of the ocean basins and is statistically significant. Hence, this particular analysis is applied only to SST.

Figure 4 shows the results for SST trend time series (Fig. 4A) and SST variability time series (Fig. 4B). The MI is higher when the trend (0.54 bits), in contrast to the variability (0.30 bits), is isolated, and the trend value is comparable to that of the original signal (0.51 bits). In addition, it can be observed that the scaled distribution of the trend is very similar to that of the original variable (Fig. 4A versus Fig. 2E). The high values of NCAT45 appear to be associated with high SST (the upper part of the diagonal) when the trend is isolated (Fig. 4A); however, this is not the case for the variability, which is very symmetrical around the median (Fig. 4B). This implies statistically that the trend in SST accounts for the information associated with the occurrence of high values of NCAT45, whereas the shorter-term variability in SST does not account for a

large proportion of the variance of the high NCAT45.

Recently, the quality of the hurricane data has been questioned (*4*, *5*), and a reanalysis of the tropical cyclone databases has even been suggested in order to confirm that the results of recent studies (*1*, *2*) are not due to problems in the data. Because the NIO hurricane data set has been directly questioned because of potential problems, especially during the 1970s, we performed the MI analysis excluding this basin, obtaining similar results pointing to the same conclusions reached when all six basins were used (fig. S4). In addition, we analyzed the behavior of the seasonal tropospheric moist static stability for all six basins. We found a statistically significant and strong negative trend in this variable for five of the six basins (fig. S5), indicating a more unstable troposphere. Interestingly, although the EPAC shows no trend in the moist static stability index, it is the only basin that presents a significant positive trend in the specific humidity (Table 1). These results support the physical connection between ocean and atmosphere for the link between increasing SST and NCAT45.

An outstanding issue is to investigate whether the SST variation is the primary source of information shared with the NCAT45 trend in the three basins that possessed statistically significant trends in other variables: the EPAC specific humidity, the SPAC stretching deformation at 850 mb, and the NATL vertical wind shear. Because the number of data points for each basin is only 35, we could not apply the MI technique. Hence, we conducted a correlation analysis on the complete and detrended time series for each of these basins (Table 2). The correlation between humidity and NCAT45 in the EPAC is not statistically significant. The correlation between stretching deformation and NCAT45 in the SPAC is statistically significant, but the correlation arises almost entirely from the short-term internal variability. The correlation between wind shear and NCAT45 in the NATL is statistically significant, but the correlation is dominated by the short-term variability.

Unfortunately, the sample size for the individual basins is too small to reliably test the significance of the difference between the correlation for the original time series and that for the detrended time series. The same correlation analysis shown in Table 2 for SST (*18*) reveals that the correlation for SST in the original time series is more than twice as large as for the detrended time series. This analysis suggests that the only basins where there may be some significant contribution of trend from variables besides SST are the NATL and the SPAC. Although this analysis cannot determine quantitatively the relative contributions of SST versus vertical wind shear to the NCAT45 trend in the NATL and versus zonal stretching deformation in the SPAC, the relative differences in the magnitudes of correlations for the complete versus the detrended time series indicate that the contribution from SST dominates in both basins in contributing to the trend in NCAT45.

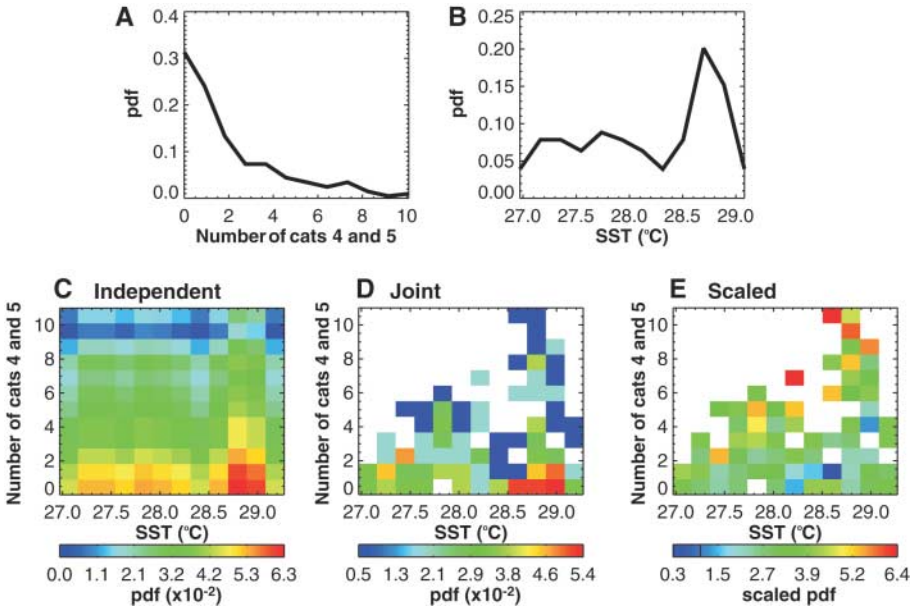

Fig. 2. Marginal distributions in all basins for (**A**) NCAT45 and (**B**) SST. pdf, probability density function. (**C**) Product of the marginal distributions, (**D**) joint distribution, and (**E**) scaled distribution for (A) and (B).

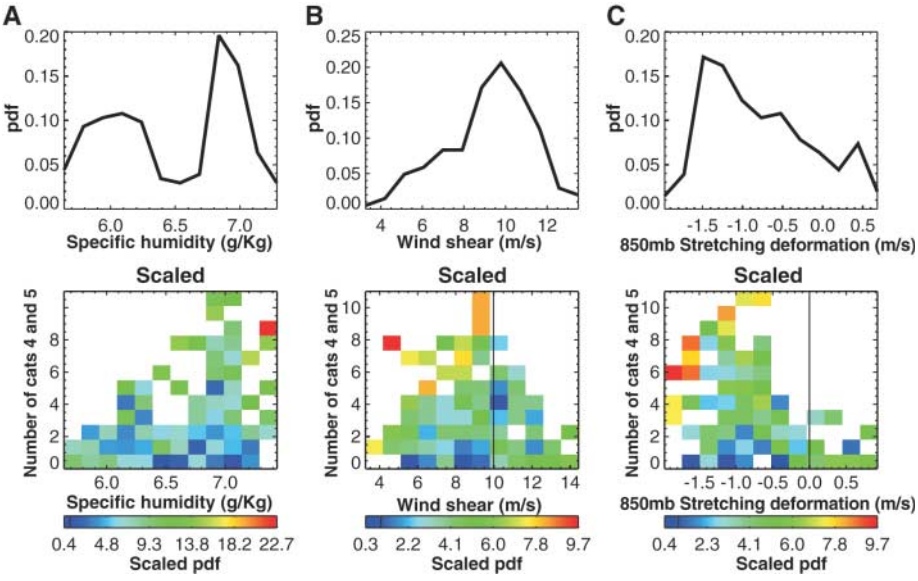

Fig. 3. (**A** to **C**) Marginal and scaled distribution for (B) to (D) in Fig. 1. The vertical black line in the bottom panels of (B) and (C) corresponds to the median of the distribution in (B) and to zero in (C).

Our results show that seasonally averaged values of tropical SST, tropospheric humidity, vertical wind shear, and zonal stretching deformation share information content with the total number of NCAT45 in a season. The shared information content with tropospheric humidity, vertical wind shear, and zonal stretching deformation is dominated by short-term variability, whereas the shared information content with SST is dominated by the longer-term trend. The implication of these results is that the strong increasing trend in NCAT45 for the period 1970–2004 is directly linked to the trend in tropical SST, and that other aspects of the tropical environment, although they influence shorter-term variations in hurricane intensity, do not contribute significantly to the global trend of increasing hurricane intensity. We infer that there is some contribution to the long-term trend from wind shear in the NATL and from stretching deformation in the SPAC, but that the contribution from SST remains dominant in these basins in contributing to the trend in NCAT45.

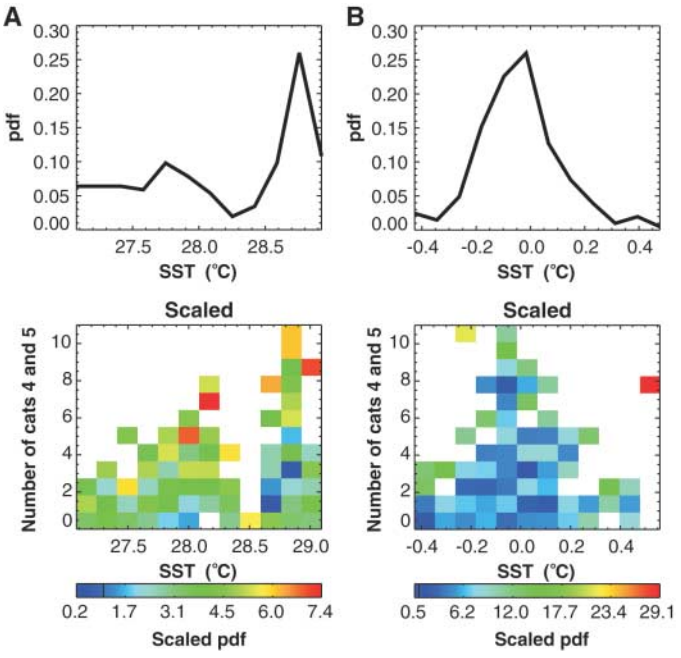

Fig. 4. Marginal and scaled distribution for (**A**) the SST trend time series and (**B**) the detrended SST variability time series. Values greater than one (the vertical line in the color bar at the bottom) account for the MI shared between the variables.

Table 2. Correlations for individual ocean basins between NCAT45 and variables for which there is a statistically significant trend in that basin, for the original time series in bold and the detrended time series in parentheses. NA, not applicable.

Variable	EPAC	NATL	SPAC
SST	**0.32*** (0.06)	**0.67*** (0.20)	**0.29** (–0.10)
Specific humidity	**0.23** (0.13)	NA	NA
Wind shear	NA	**–0.61*** (–0.45)*	NA
Stretching deformation	NA	NA	**–0.67*** (–0.55)*

*Statistically significant correlations at the 95% confidence level.

References and Notes

1. P. J. Webster, G. J. Holland, J. A. Curry, H.-R. Chang, *Science* **309**, 1844 (2005).
2. K. E. Trenberth, *Science* **308**, 1753 (2005).
3. K. Emanuel, *Nature* **436**, 686 (2005).
4. C. W. Landsea, *Nature* **438**, E11 (2005).
5. K. Emanuel, *Nature* **438**, E13 (2005).
6. J. A. Curry, P. J. Webster, G. J. Holland, in preparation.
7. R. A. Pielke Jr., C. Landsea, M. Mayfield, J. Laver, R. Pasch, *Bull. Am. Meteorol. Soc.* **86**, 1571 (2005).
8. L. J. Shapiro, S. B. Goldenberg, *J. Clim.* **11**, 578 (1998).
9. P. J. Webster, G. J. Holland, R. A. Houze Jr., paper presented at the 85th American Meteorological Society Annual Meeting, the Ed Lorenz Symposium, San Diego, CA, 13 January 2005 (http://ams.confex.com/ams/Annual2005/techprogram/paper_87148.htm).
10. T. M. Smith, R. W. Reynolds, *J. Clim.* **17**, 2466 (2004).
11. E. M. Kalnay *et al.*, *Bull. Am. Meteorol. Soc.* **77**, 437 (1996).
12. R. M. Hirsch, J. R. Slack, R. Smith, *Water Resour. Res.* **18**, 107 (1982).
13. C. E. Shannon, *Bell System Tech. J.* **27**, 379 (1948).
14. Information on the statistical method is available as supporting material on *Science* Online.
15. J. Lighthill *et al.*, *Bull. Am. Meteorol. Soc.* **75**, 2147 (1994).
16. W. M. Gray, *Mon. Weather Rev.* **96**, 669 (1968).
17. Values of MI vary from 0 (total independence) to 2.8 (total dependence), corresponding to the entropy of NCAT45 (minimum among all variables).
18. SST correlations for the remaining three basins are as follows (using the same notation as in Table 2): WPAC **0.44*** (0.13), NIO **0.28** (–0.10), SIO **0.54*** (0.02).

19. This research was supported by the Climate Dynamics Division of NSF under award NSF-ATM 0328842.

Supporting Online Material

www.sciencemag.org/cgi/content/full/1123560/DC1
SOM Text
Figs. S1 to S5
Reference

7 December 2005; accepted 7 March 2006
Published online 16 March 2006;
10.1126/science.1123560
Include this information when citing this paper.

Evolution of Hormone-Receptor Complexity by Molecular Exploitation

Jamie T. Bridgham, Sean M. Carroll, Joseph W. Thornton*

According to Darwinian theory, complexity evolves by a stepwise process of elaboration and optimization under natural selection. Biological systems composed of tightly integrated parts seem to challenge this view, because it is not obvious how any element's function can be selected for unless the partners with which it interacts are already present. Here we demonstrate how an integrated molecular system—the specific functional interaction between the steroid hormone aldosterone and its partner the mineralocorticoid receptor—evolved by a stepwise Darwinian process. Using ancestral gene resurrection, we show that, long before the hormone evolved, the receptor's affinity for aldosterone was present as a structural by-product of its partnership with chemically similar, more ancient ligands. Introducing two amino acid changes into the ancestral sequence recapitulates the evolution of present-day receptor specificity. Our results indicate that tight interactions can evolve by molecular exploitation—recruitment of an older molecule, previously constrained for a different role, into a new functional complex.

The ability of mutation, selection, and drift to generate elaborate, well-adapted phenotypes has been demonstrated theoretically (*1*, *2*), by computer simulation (*3*, *4*), in the laboratory (*5*, *6*), and in the field (*7*). How evolutionary processes assemble complex systems that depend on specific interactions among the parts is less clear, however. Simultaneous emergence of more than one element by mutational processes is unlikely, so it is not apparent how selection can drive the evolution of any part or the system as a whole. Most molecular processes are regulated by specific interactions, so the lack of exemplars for the emergence of such systems represents an important gap in evolutionary knowledge. As Darwin stated, "If it could be demonstrated that any complex organ existed which could not possibly have been formed by numerous, successive, slight modifications, my theory would absolutely break down" (*8*).

The functional interaction between the steroid hormone aldosterone and its specific partner the mineralocorticoid receptor (MR)—a ligand-activated transcriptional regulator (*9*, *10*)—illustrates this evolutionary puzzle. MR and the glucocorticoid receptor (GR) descend from a gene duplication deep in the vertebrate lineage (*11*) and now have distinct signaling functions. In most vertebrates, GR is specifically activated by the stress hormone cortisol to regulate metabolism, inflammation, and immunity (*9*). MR is activated by aldosterone to control electrolyte homeostasis and other processes (*9*, *12*). MR can also be activated by cortisol, although the presence of a cortisol-

Center for Ecology and Evolutionary Biology, University of Oregon, Eugene, OR 97403, USA.

*To whom correspondence should be addressed. E-mail: joet@uoregon.edu